100 Gbps/ PON downstream O- And C-band alternatives using direct-detection and linear-impairment equalization [Invited]

100 Gbps/λ PON downstream O- and C-band alternatives using Direct Detection and Linear-Impairments Equalization [Invited]

PABLO TORRES-FERRERA[1,*], HAOYI WANG[1], VALTER FERRERO[1], ROBERTO GAUDINO[1]

[1] *Politecnico di Torino, Department of Electronics and Telecommunications, Torino (TO), Italy*
**Corresponding author: pablo.torres@polito.it*

Received XX Month XXXX; revised XX Month, XXXX; accepted XX Month XXXX; posted XX Month XXXX (Doc. ID XXXXX); published XX Month XXXX

Future generation Passive Optical Networks (PON) physical layer, targeting 100 Gbps/wavelength, will have to deal with severe optoelectronics bandwidth and chromatic dispersion limitations. In this paper, largely extending our Optical Fiber Communications Conference (OFC) 2020 invited paper, we review 100 Gbps/ wavelength PON downstream alternatives over standard single-mode fiber in O- and C-bands, analyzing three modulation formats (PAM-4, Partial-Response PAM-4 and PAM-8), two types of direct-detection receivers (APD- and SOA+PIN-based) and three digital reception strategies (un-equalized, feed-forward equalized and decision-feedback equalized). We evaluate by means of simulations the performance of these alternatives under different optoelectronics bandwidth and dispersion scenarios, identifying O-band feasible solutions able to reach 20 km of fiber and an optical path loss of at least 29 dB over a wide wavelength range of operation. Finally, we compare two digitally pre-compensated modulation schemes that are highly tolerant to chromatic dispersion, showing a possible extension to C- band operation preserving direct-detection and linear impairments equalization at the Optical Network Unit side.

http://dx.doi.org/10.1364/JOCN.99.099999

1. INTRODUCTION

The rapid traffic growth in the access network segment has driven the development of faster Passive Optical Networks (PON). Next-generation 25 Gbps and 50 Gbps single-wavelength (λ) PON solutions are in advanced standardization status [1-5]. In fact, the IEEE P802.3ca 50G-EPON Task Force has recently released the IEEE Std 802.3-2020 standard [1], defining specifications for 25 and 50 Gbps Ethernet PON, based on 25 Gbps/λ O-band technology. Currently, the development of 100 Gbps/λ PON (100G-PON) alternatives is a very active research topic [6-19], as shown in many papers on this topic published at the recent Optical Fiber Communications Conference (OFC) 2020. The present contribution is an extension of our invited paper presented at that Conference [20], and it discusses some physical layer options to implement 100G-PON in the downstream (DS) direction, giving first a review of the existing literature, and then presenting the specific proposals arising from our activities in the field. While in our OFC 2020 paper [20] we focused mostly on the 50G-PON solution, in this extended version we completely move the focus towards 100 Gbps/λ PON.

New PON upgrades to higher speed tend to re-use optoelectronic (O/E) technology developed for the data center interconnects (DCI) realm [6]. However, there are two key differences between PON and DCI (as well as other similar short-reach systems): the much higher optical path loss (*OPL*) and longer fiber reach (of at least 20 km) requirements of the former. Consequently, from a physical layer perspective, the evolution from 50G-PON to 100G-PON has to face the following well-known three main challenges:

1. A limited available bandwidth (*BW*) in the O/E devices to support the required bit rate (R_b) while keeping low the format cardinality to avoid sensitivity penalties.
2. An increased impact of chromatic dispersion (CD).
3. A more severe impact of the accumulation of different noise sources.

Regarding the first point, which is likely the most severe one when upgrading to 100G-PON, nowadays O/E technology with the required *BW* to support 100 Gbps/λ direct on-off keying (OOK) transmission is not mature enough, thus not commercially available. Therefore, alternatives to enable operation using bandlimited technology should be considered, such as digital signal processing (DSP) to use higher order modulation formats and/or adaptive equalization (AEQ). For

instance, using quaternary pulse amplitude modulation (PAM-4) helps on reducing the baud rate (R_S) to 50 GBd allowing operation with upcoming 50G-class O/E technology (50G-OE). Another alternative is the re-use of existing 25G-class O/E technology (25G-OE), with PAM-4 or even higher-cardinality formats, in combination with AEQ. To enable DSP functionalities, analog-to-digital and digital-to-analog converters (ADC and DAC, respectively) are needed, which nowadays poses another constraint to 100 Gbps OOK viability, considering that AEQs typically require 2 samples per symbols (SpS) operation (i.e. 200 GSpS). The use of DSP to compensate for *BW* limitations in high-speed PON has been studied in many scientific papers, including previous contributions of our group [20-22] in which this important PON limitation was analyzed in detail for the 25G- and 50G-PON scenarios.

Moving to the second challenge, i.e. how to deal with the CD penalty issue, the following alternatives have been considered so far (the first four preserving the conventional direct-detection (C-DD) scheme):

i) O-band operation (i.e. around 1330 nm): 25G- and 50G-PON standardization processes have considered this option, since C-DD receivers would not work in C-band. Very recent works have demonstrated 100G-PON feasibility over at least 20-km in O-band using PAM-4 and bandlimited devices [7, 8].

ii) Coding against CD: it has been shown that a combination of coding and pulse shaping, generating a proper digital pre-chirping condition, allows increasing the signal robustness to CD [23-25]. One technique of this type is Combined Amplitude Phase Shift (CAPS) codes [24], which moreover can be detected with a conventional OOK receiver (RX). A simplified version of CAPS order 3 is called IQ-duobinary (IQ-DB) [24, 25], which helps reducing significantly the transmitter (TX) complexity at the cost of a small CD robustness reduction. IQ-DB has been proven effective to extend the C-band operation to ~17-km in a 50 Gbps experimental transmission [25], using a C-DD OOK un-equalized RX and a dual-arm IQ Mach-Zehnder Modulator (IQ-MZM).

iii) CD Digital Pre-Compensation (CD-DPC) [26-29]: the link accumulated dispersion is digitally pre-compensated at the TX, so that (at least in an ideal linear regime) the RX signal is unaffected by CD and can thus be DD received. This DS solution adds reasonable complexity to a C-DD system, but only at the Optical Line Terminal (OLT) side, while the Optical Network Unit (ONU) is unaffected. In [9], our group proposed this solution for the 100G-PON DS scenario over up to 20-km in L-band sticking to C-DD RX and simple DSP at ONU side, using PAM-4, simple FIR filter processing and an IQ-MZM. In [29] we extended this analysis including experimental demonstrations for 50, 100 and 125 Gbps operation, over 25 and 50 km in C-band.

iv) Neural networks or Machine learning pre- or post-equalizers: Very recently, some pioneering works have demonstrated 100 Gbps C-band solution on a C-DD approach using nonlinear adaptive equalizers based on neural networks [16-18]. However, the DSP complexity is enormous and it would require a major upgrade in DSP chipsets.

v) Single sideband (SSB) advanced modulation coupled with Kramers-Kronig (KK) RX [15, 30]: this alternative may have severe drawbacks for PON since it usually does not provide a significant sensitivity gain as compared to a C-DD RX (since a strong unmodulated optical carrier must be transmitted along with the modulation signal in the KK self-coherent approach avoiding a local oscillator at RX) and its required RX electronic BW compared to a C-DD RX at the same rate is usually higher (KK RX is very sensitive to O/E *BW* limitations [30]). Moreover, at least in the basic version, KK DSP require an important over-sampling factor compared to a C-DD RX DSP, which poses a major cost issue for 100 Gbps/λ operation.

vi) Advanced modulation formats and coherent detection with electronic DSP [10-15]: this option solves any reasonable transmission problem for the foreseeable future, but its use in the PON area is still uncertain, due to complexity, cost and power consumption increase of both the TX and RX hardware [6, 7, 15].

One important PON design target is maintaining the ONU complexity as low as possible, putting more complexity at the OLT side if needed. Then, in the downstream (DS)/upstream (US) direction, a simple RX/TX is desired and a more complex TX/RX can be accepted. From the previous listed 100G-PON alternatives, the option *i*) can work in both DS and US directions, just considering the burst-mode power penalty in the US power budget, since it is a direct extension of 25G- and 50G-PON O-band systems, already demonstrated feasible in both directions. We consider that 100G-PON C-band alternatives are worth to be studied, because they match better with future PON long-reach system requirements and we can envision that by the time 100G-PON will be needed, operators would have already replaced current C-band PON systems (such as G- and XGS-PON) by upcoming O-band ones (like 25G- and 50G-PON), thus freeing the C-band spectrum [29]. 100G-PON C-band alternatives *iv)*, *v)* and *vi)* put considerable complexity at the RX side, thus being more appropriate for the US conditions. In fact, coherent-based C-band solutions have been proven feasible in burst-mode (BM) operation [10, 12, 13], and in continuous mode (CM) preserving intensity modulation (IM) at TX side [11], achieving a sensitivity, *OPL* (at $BER=10^{-2}$) and maximum reach of -32.5 dBm, 33.5 dB and 40 km (BM) in [10, 12]; -26 dBm, 34 dB and 40 km (CM) in [11]; and -41.5 dBm, 37.5 dB and 50 km (BM) in [13], respectively. Regarding the DS direction, 100G-PON alternatives able to avoid complex [15] and costly [6] RX at the ONU side (i.e. coherent-detection, KK-RX or nonlinear equalization) have been less analyzed [9, 15, 29]. Therefore, focus of this contribution is studying C-DD solutions in this realm.

In [20], our group presented a selection of our last two years works on 25G- and 50G-PON C-DD bandlimited solutions aided by equalization and using OOK, Duobinary (DB) and PAM-4 formats in O-band. An extensive update is given in this new contribution, which explores by means of simulations the performance of 100G-PON DS alternatives keeping the C-DD approach at the ONU while maintaining a reasonably low DSP complexity. We start by considering a typical IM-DD system targeting O-band operation in a standard single-mode fiber (SMF). Three modulation formats are considered: PAM-4, which has been demonstrated feasible under this scenario so we use it as a baseline, Partial Response PAM-4 (PR-PAM-4, a sort of "duobinary PAM-4"), and PAM-8. The last two formats are more resilient to CD than PAM-4, so that we study them as an alternative to increase the λ-range of operation inside the O-band.

The IM-DD analysis, both in BtB (to study the *BW* limitations impact in the absence of dispersion) and over SMF (to study the impact of fiber propagation in extended O-band), is the core part of our contribution. In addition, in the last part of the paper, we explore the possibility of enabling C-band transmission by using *i*) the aforementioned CD-DPC technique in combination with PAM-4, PR-PAM-4 and PAM-8 formats, or *ii*) the so-called IQ-DB scheme in the electrical and optical versions.

Regarding the receiver, two different C-DD schemes are compared in our paper: an avalanche photodiode (APD) and a PIN photodiode preceded by a semiconductor optical pre-amplifier (SOA). The system performance achieved when using nominal 50G-OE or 25G-OE is also compared considering three different digital RX types: *i*) avoiding equalization (No EQ), *ii*) using feed forward equalizer (FFE) or *iii*) using FFE followed by a decision feedback equalizer (DFE). To keep complexity under reasonable limits for the ONU, we avoid including more complex equalizers meant to compensate for non-linear impairments, like the aforementioned neural-network based equalizers. Moreover, we also avoid using TX pre-equalization, since it has been shown that it does not outperform RX post-equalization (which it is also simpler from a network operation point of view) and it

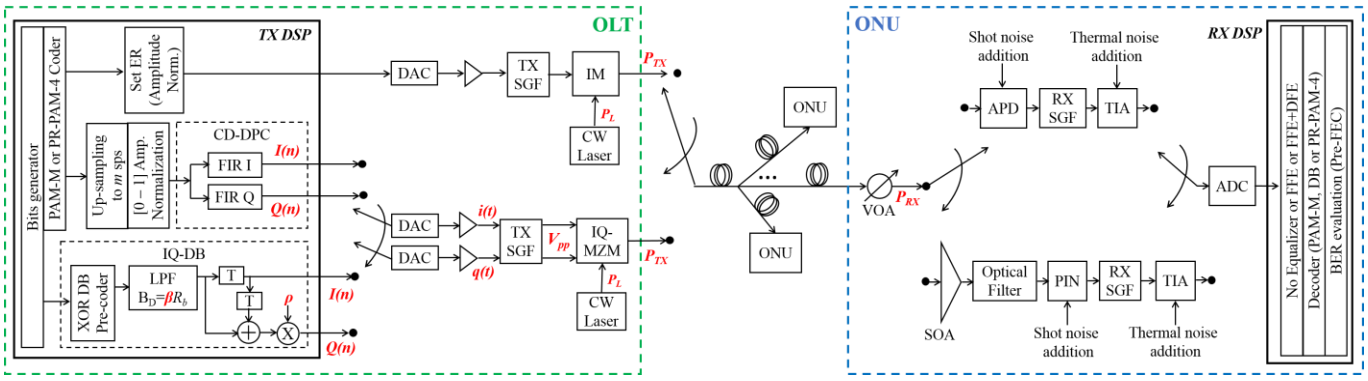

Fig. 1. Simulation setup. The total fiber length L is measured from the output of the optical transmitter to the input of the VOA at the RX.

provides only very small performance gain if combined with post-equalization when linear-impairments are corrected [31].

The paper is organized as follows: in Section 2, the simulation setup and the different studied architectures are described, then in Section 3 we present our back-to-back (BtB) results about the impact of *BW* limitations and equalization. In Section 4, we analyze the impact of fiber propagation in the performance of the different transmission scenarios. Finally, we conclude and discuss our work in Section 5.

2. SIMULATION SETUP

The simulation setup is shown in Fig. 1, which summarizes all the TX and RX options that we analyze in the rest of the paper. For O-band operation, we consider the use of a traditional IM optical transmitter without any TX DSP dispersion pre-compensation (architecture 1, so-called "IM-DD"). For C-band operation, we compare two TX schemes using an IQ-MZM. One uses a CD-DPC technique [9, 29] that emulates in the digital domain the propagation over a linear SMF with the same accumulated dispersion ($D{\cdot}L$) of the link but with opposite sign (architecture 2, so-called "CD-DPC-DD"). The other uses a technique called IQ-DB [24, 25] that adds digitally a given amount of chirp to counteract a given amount of dispersion (architecture 3, so-called "IQ-DB-DD"). At the receiver side, conventional direct-detection is employed with or without adaptive equalization. The details of the simulator and the employed parameters are provided below.

A. Transmitter

1. IM-DD architecture

A random bit sequence is coded to generate a rectangular-shaped PAM-4, PR-PAM-4 or PAM-8 signal, which drives a bandlimited intensity modulator (IM) after DAC conversion and proper amplitude normalization to set the extinction ratio (ER). The PR-PAM-4 sequence is obtained after pre-coding a PAM-4 sequence following the rule: $b(k) = (a(k) - b(k\text{-}1)) \bmod 4$, where $a(k)$ are the original PAM-4 symbols, and $b(k)$ are the 4-level pre-coded symbols [32]. In the conventional approach, the pre-coded sequence is typically encoded to obtain the 7-level PR-PAM-4 sequence $c(k)$ with an add-and-delay digital filter (ADDF) as follows: $c(k)=b(k)+b(k\text{-}1)$ [32, 33]. It is know that the ADDF can be well approximated (thus replaced) to a 5th order Bessel filter with a cut-off frequency of around 30% of the baud rate [19]. In the PR-PAM-4 approach used here, the pre-coded sequence is sent without encoding, using in our favor the inherent O/E channel filtering to help generating the 7-level PR-PAM-4 at the RX side (in fact, the PR-PAM-4 received eye-diagrams look exactly the same as the PAM-4 ones before equalization, as shown in bottom of Fig. 4), under proper *BW* conditions and right sampling instant choice. Apart from correcting linear channel distortion, a RX equalizer trained with a PR-PAM-4 encoded sequence can be employed to enforce the required frequency response that generates the proper 7-level PR-PAM-4 sequence. This PR-PAM-4 option is more convenient than the conventional one in equalized bandlimited systems with 3-dB bandwidth around 0.3 times the baud rate (~15 GHz transmitting a pre-coded 100 Gbps PAM-4 signal), since part of the *BW* limitations are not prejudicial but helpful, and therefore the amount of distortion that should be compensated by the equalizer is relaxed, improving the performance. The spectra of the transmitted PAM-4 original sequence $a(k)$ and the pre-coded PAM-4 sequence $b(k)$ (to generate PR-PAM-4) are identical. After channel filtering and equalization, the PR-PAM-4 signal spectrum becomes narrower than the PAM-4 one [33]. The spectrum of the PAM-8 signal is even narrower, having a Nyquist frequency 33% smaller than that of PAM-4 [34] . These facts are useful to be considered to follow the discussion of the results presented in Section 3 about the impact of bandwidth limitations.

2. CD-DPC-DD architecture

The bit sequence is coded to generate a PAM-4, PR-PAM-4 or PAM-8 signal, which is up-sampled to 2 samples per symbol (SpS), and its amplitude is normalized between 0 and 1. The normalized signal is filtered using a pair of 80-taps FIRs filters to perform the CD pre-compensation described in details in [9, 29]. The taps of the "*FIR I*" and "*FIR Q*" are evaluated as indicated in Equations (27) and (28) in [35], allowing "short" filters even for the high $D{\cdot}L$ values tested here. Basically, this approach pre-compensate CD in the electronic DSP domain. The I and Q signals that outputs the CD-DPC block drive an IQ-MZM after DAC conversion and electrical amplification. For high accumulated dispersion, the I and Q signal amplitude distributions are approximately Gaussian, but their peak-to-peak amplitude (V_{pp}) and mean value are different: the Q mean is around zero, while the I one is around 0.5, when the input signal is normalized between zero and one. This fact is relevant to properly drive the IQ-MZM, by optimizing the V_{pp} driving signals and the modulator bias, which directly affects the optical modulation index (OMI) and the IQ-MZM linearity. The V_{pp} is set by amplifying the driving signals (after mean removal) with the same gain factor so that no IQ imbalance is introduced (however their V_{pp} is different, since they have different amplitude at the output of the CD-DPC, as mentioned before). The modulator I- and Q-arms are biased at quadrature and null, respectively.

3. IQ-DB-DD architecture

The bit sequence is pre-coded as follows: $b(k) = (a(k) - b(k\text{-}1)) \bmod 2$, where $a(k)$ are the original bits, and $b(k)$ are the pre-coded binary symbols [32]. The mod 2 operation is typically performed using an XOR gate. The resulting signal is low-pass filtered using a 5th order Bessel filter with a 3-dB bandwidth (B_D) equal to $\beta{\cdot}R_b$, where β is a parameter to optimize, to produce a 3-level DB sequence $s(k)$ [24]. The I and Q DB-

signals are obtained as follows: $I(k)=s(k\text{-}1)$ and $Q(k)=\rho(s(k)+s(k\text{-}2))$, where ρ is a parameter to be optimized [24]. After DAC conversion and electrical amplification (setting a proper V_{pp} amplitude), the IQ-DB output signals drive an IQ-MZM, whose I and Q arms are biased in quadrature or null whereas electrical or optical DB version is used, respectively.

B. Propagation and detection

The modulated optical signal is launched into a conventional G.652 SMF. At the RX side, a variable optical attenuator (VOA) is used to set the *OPL*. Then, the signal is converted into the electrical domain using one of the two C-DD optical receivers considered in our study: an APD one or an SOA+PIN one (with an optical filter in between). The optical RX output signal is digitized and processed, using one of the following digital RX options: *i*) without equalization, just setting the optimum sampling instant and thresholds for symbol decision, *ii*) with equalization: 20-taps FFE or *iii*) with equalization: 20-taps FFE + 5-taps DFE (termed by simplicity just as "DFE" in the rest of the manuscript). The AEQs are trained using 10^4 symbols and then switched to tracking (decision-directed) mode. After proper symbol decision and decoding, the bit error ratio (*BER*) is evaluated through error counting over 10^5 bits.

In the case of PR-PAM-4, the received sequence after decision $d(k)$ is first converted into PAM-4 symbols $\hat{a}(k)$, for decoding, as follows: $\hat{a}(k) = d(k) \bmod 4$ [19]. Note that $d(k)$ is meant to be a 7-level encoded signal after channel filtering (and in combination with equalization when applied), as explained before.

When IQ-DB in electrical flavor is employed, the received sequence $d(k)$ is converted to bits again as follows: $\hat{a}(k) = d(k) \bmod 2$, where $d(k)$ is meant to be a 3-level sequence after channel filtering (and in combination with equalization when applied) [22]. Whereas the IQ-DB in optical version is used, the received electrical sequence is already binary, thus digital DB decoding is not needed (the DB decoding is already performed by the optical to electrical conversion [21]).

C. Simulation models and main parameters

The SMF is modeled using the conventional non-linear Schrodinger equation (NLSE) solved numerical by the split-step Fourier method. The SMF parameters in C-band (O-band) at a reference wavelength λ=1550 nm (λ=1342 nm) are: chromatic dispersion coefficient D=17 ps/(nm·km) (D=4 ps/(nm·km)), attenuation of 0.22 dB/km (0.5 dB/km), effective area of 80 μm^2 and nonlinear index of $26\text{x}10^{-21}$ m^2/W. To emulate the TX and RX physical frequency response, we used 2nd order low-pass super-Gaussian filters (SGF) [21, 22], with a given -3dB BW (f_{3dB}), set the same at the TX and RX SGFs depending on the employed O/E technology: f_{3dB} = 18.75 GHz for 25G-OE and f_{3dB} = 37.5 GHz for 50G-OE. The DAC and ADC blocks have a resolution of 6 bits for quantization, and are used to up-sample the TX signal and down-sample the RX one, respectively, in order to use a higher sampling frequency of $32{\cdot}R_S$ GS/s (i.e. 32 SpS) for a numerically accurate simulation of the fiber propagation and the analog transfer functions of the O/E channel blocks. The IM is assumed linear and chirp-less with an ER=8 dB [5], an average transmitted power of P_{TX} = 11 dBm [8] and a relative intensity noise (RIN) of -150 dB/Hz. Externally modulated lasers (Electro-absorption Modulated Laser (EML) and MZM) have been preferred over directly modulated lasers (DML) for single-λ 50G-PON solutions [5, 6, 36, 37], since DMLs typically have less ER [6] and O/E bandwidth, and generate more chirp [38]. A generic IM is considered here, that can model both a MZM and an EML provided that they are low-chirp devices and operated in linear regime (reasonable assumption for the target ER). Whereas the MZM is certainly a low-chirp device (but more expensive [6, 38]), the EML can generate a non-negligible amount of chirp. The impact of the EML chirp in an IM-DD single-λ 50G-PON system is analyzed in detail in [36], showing that the feasible wavelength range of operation can be shifted depending on the amount (and sign) of chirp, as discussed later for the IM-DD system analyzed here. The IQ-MZM model assumed a squared cosine voltage-to-power conversion characteristic with equal power distribution into the arms. We set the IQ-MZM static insertion loss equal to 7 dB plus a dynamic modulation loss that depends on the driving signals V_{pp}. The continuous wave (CW) laser that feeds the IQ-MZM has a power of P_L=21 dBm (for CD-DPC-DD) or P_L=19 dBm (for IQ-DB-DD). Under these conditions the IQ-MZM output power is around P_{TX} = 11 dBm (the exact P_{TX} depends on the driving signals V_{pp}). The RX SOA is assumed linear with gain G = 15 dB and noise figure equal to 7.5 dB. The SOA input powers, when used as a pre-amplifier in PON systems, are typically lower than standard SOAs saturation power. In our simulations, SOA input powers in the range of -12 to -24 dBm are analyzed, which results in SOA output powers in the range of -9 to +3 dBm (for G = 15 dB), far enough from a typical SOA saturation output power of ~8.5 dBm. Therefore, we consider that the SOA linear model is accurate enough for our purposes, and very small penalties due to preamplifier SOA nonlinearities can be expected for a practical PON implementation. The optical filter, placed at the SOA output, has a pass-band of 75 GHz, modelled as a 5th order SGF, emulating the DWDM filters envisioned for the TWDM-PON standard. The optical RX parameters for 25G-OE technology are: APD multiplication gain M = 8, APD excess noise factor F = 6.36 dB (ionization factor of 0.4), PIN/APD responsivity R = 0.8 A/W, and intensity referred noise density (*IRND*) of 10 pA/sqrt(Hz) [5]. The corresponding parameters for 50G-OE are: APD M = 5, F = 4.88 dB (ionization factor of 0.4), PIN/APD R = 0.7 A/W and *IRND* = 15 pA/sqrt(Hz) [5]. The shot and thermal noise sources at the RX are modelled as additive white Gaussian noise random processes [21, 22], with variance evaluated as follows: $\sigma_{sh}^2 = 2FM^2qB_sRP_i(t)$ and $\sigma_{th}^2 = B_s \cdot (IRND)^2$ respectively (M and F are equal to 1 if PIN is used). B_s is the one-sided simulation bandwidth, q is the electron charge and $P_i(t)$ is the instantaneous PIN or APD input optical power. The receiver parameters are assumed to be the same in O- and C-bands.

The system performance parameters used as figures of merit are: the *BER*, the average received optical power measured at the VOA output (*ROP*) that is required (*RROP*, sometimes called "sensitivity") to obtain a given *BER* target (chosen $BER_T=10^{-2}$ [4]), and the achievable *OPL* that guarantees operation equal or below the BER_T (*OPL* is sometimes termed as *ODN* loss, calculated as the difference in dB between the average transmitted power P_{TX} and the *ROP* in dBm) All the gain and power penalties are referred to BER_T, i.e. measured as the difference in dB between the compared *RROP* values or achievable *OPLs*.

3. IM-DD BACK-TO-BACK RESULTS

In this Section, we report the simulation results obtained in back-to-back (BtB) conditions using the IM-DD architecture. A comparison between modulation formats, and optical and digital receiver options is performed. Nominal parameters are considered for 25G-OE (based on component vendor inputs [5]), whereas parameters for 50G-OE are chosen based on reasonable forecasts considering some reduction in the device performance (higher *IRND* and lower R and M) when increasing the bandwidth from around 18.75 GHz (25G-OE) to around 37.5 GHz (50G-OE) [5] (see sub-section 2.C).

A. IM-DD with 50G-class optoelectronics (50G-OE) technology

When using 50G-OE, a limited penalty due to bandwidth limitations for PAM-4 (R_S = 50 GBd) and PAM-8 (R_S = 33.3 GBd) is expected. In contrast, for the PR-PAM-4 approach used here (R_S=50 GBd, see sub-section 2.A.1), a bad performance in broadband conditions is anticipated since a proper amount of O/E filtering is required when

equalization is not employed. When equalization is introduced, the absence of the required O/E BW limitations is compensated by properly training the AEQ to deliver a 7-level encoded PR-PAM-4 signal.

BER curves as a function of *ROP* are shown in Figures 2.a (for SOA+PIN) and 2.b (for APD), comparing different formats and digital RX options in combination with 50G-OE. As expected, the difference between the un-equalized and equalized approaches is small for PAM-4. In contrast, for PAM-8 and PR-PAM-4, there is a not negligible penalty for avoiding AEQ. In the case of PAM-8, this ~2dB penalty arises from the fact that increasing the O/E BW beyond $0.7 \cdot R_S$ (~23 GHz) does not contribute to further reduce linear distortions, but to introduce more noise to the RX. In the case of PR-PAM-4, this penalty (~4 dB) is caused due to not compensated sub-optimal filtering conditions, as mentioned in the previous paragraph. In all cases, the use of DFE provides a marginal gain as compared to FFE. A summary of the achievable *OPL* of the analyzed cases presented in Fig. 2 is reported in Table I, assuming a P_{TX} = 11 dBm (an achievable value using an EML integrated with a SOA [8]). In BtB the IM-DD simulated system is practically power independent (except for shot noise addition that anyway is not a dominant effect), then the *OPLs* of Table I can be linearly scaled to other P_{TX} values. The SOA+PIN approach has always a power gain as compared to the APD one, which depends on the format and RX type, going from 0.9 dB (for PAM-8 with FFE or DFE) to up to 2.6 dB (for PAM-4 without equalization). Note that an integrated SOA+PIN receiver is more expensive than an APD one (besides of requiring an optical filter, a SOA+PIN is ~3-4 times more expensive than a single PIN [39], whereas the APD is just ~2-3 times [40]). On the other hand, 25G- and 50G-O/E SOA+PIN technology is more mature than APD one, since the former has already been mass produced for data center applications.

An intrinsic sensitivity penalty of PR-PAM-4 and PAM-8 with respect to PAM-4, due to their higher number of symbol levels, is evident, which is one of the reasons to favor PAM-4 when 50G-OE is employed. Another reason is that PAM-4 can provide an *OPL* ≥ 29 dB (at least in BtB) even if avoiding equalization.

In [15], the performance of a 100G-PON system, using PAM-4 and 50G-OE with linear equalization is evaluated through simulations, reporting a BtB sensitivity at $BER_T=10^{-2}$ of -22.5 and -21.7 dBm when SOA+PIN and APD optical receiver is used, respectively. Similar sensitivity values equal to -22.2 dBm using SOA+PIN and -20.2 using APD, are reported in this work under similar conditions (except that APD M = 8 and *IRND* = 10 pA/sqrt(Hz) are set in [15], whereas more conservative values M = 5 and *IRND* = 15 pA/sqrt(Hz) [5] are used in the present contribution) .

B. IM-DD with 25G-class optoelectronics (25G-OE) technology

We analyze now the results obtained using 25G-OE. For PAM-4, strong *BW* limitations are present in this scenario, therefore the advantages of more powerful equalization can be anticipated. In contrast, a good performance under this *BW* conditions is expected for

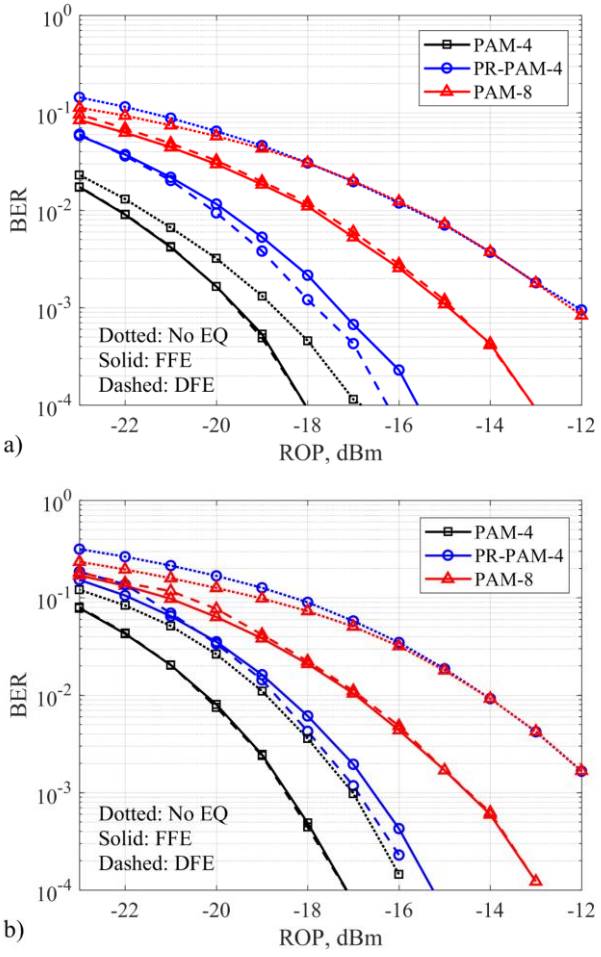

Fig. 2. BtB *BER* as a function of *ROP* comparing different formats and digital receivers in combination with 50G-class O/E devices using a) a SOA+PIN and b) an APD.

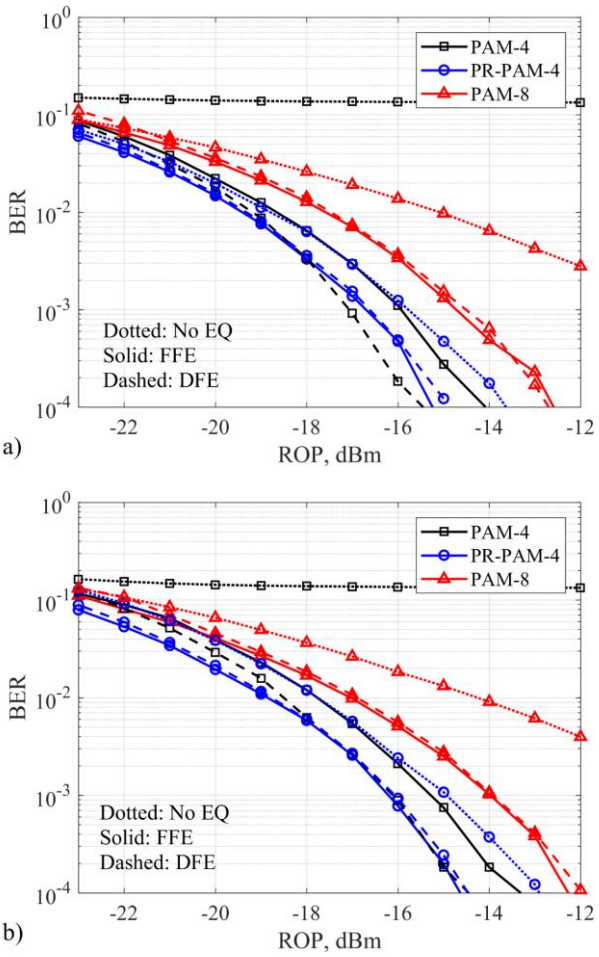

Fig. 3. BtB *BER* as a function of *ROP* comparing different formats and digital receivers in combination with 25G-class O/E devices using a) a SOA+PIN and b) an APD.

PR-PAM-4, even without equalization (the required BW limitations for PR-PAM-4 are in the order of $R_S/3$ = 17 GHz, close to the O/E BW of the cascade of a TX and RX with f_{3dB} = 18.75 GHz each).

In Figures 3.a and 3.b, we show *BER* versus *ROP* curves for SOA+PIN and APD, respectively, comparing different formats and digital RXs in combination with 25G-OE. The use of AEQ enables PAM-4 operation (without it, it does not work at all), enhancing the performance when DFE is included. In contrast, DFE does not provide any gain with respect to FFE operation in combination with PR-PAM-4 or PAM-8. Interesting to note is that PR-PAM-4 plus FFE and PAM-4 plus DFE perform very similar. A similar situation is observed when comparing PR-PAM-4 without equalization and PAM-4 with FFE, showing the adequate performance of PR-PAM-4 under the proper bandlimited conditions. A summary of the achievable *OPL* for the analyzed cases presented in Fig. 3 is reported in Table I, assuming P_{TX} = 11 dBm.

In order to extend the analysis of the impact of filtering on the system performance using different formats and digital RX, we tested different TX and RX f_{3dB} values around the already analyzed ones (i.e. 18.75 GHz for 25G-OE and 37.5 GHz for 50G-OE). Identical TX and RX filters are assumed (i.e. having same f_{3dB} and shape). In Fig. 4, achievable *OPL* curves as a function of f_{3dB} are plotted under different scenarios, using SOA+PIN (we verified that the APD results look very similar, just updating the y-axis levels). Except for the f_{3dB}, the rest of the parameters were set fixed, equal to the nominal ones for 25G-OE (then, the 50G-OE features are slightly enhanced). We observed that the performance is very stable in the 50G-OE range, irrespective of the format and digital RX type. The situation is very different in the 25G-OE domain. In this area, and including AEQ, PAM-8 exhibits the more stable performance, followed by PR-PAM-4 (a 0.8 and 1.5 dB *OPL* excursion is measured). However, PR-PAM-4 outperforms PAM-8 over the full 25G-OE f_{3dB} range. PAM-4 performance is very sensitive to f_{3dB} variations inside this region (4 dB and >10 dB *OPL* excursions are measured using DFE and FFE, respectively). When AEQ is avoided, the only format that is feasible in the 25G-OE area is PR-PAM-4. However, proper *BW* conditions should be guaranteed, otherwise a big penalty can arise. Un-equalized PAM-8 is the worst performing format using both 25G- and 50G-OE, so that we do not analyze this option in the rest of the manuscript.

In [8], the performance of an APD-based system, using 25G-OE and PAM-4 plus FFE or DFE is experimentally tested, reporting a 100 Gbps BtB sensitivity of -20 dBm at BER_T=10^{-2} using 135-taps FFE. The BtB sensitivity obtained under similar conditions (but with only 20-taps FFE) in this work is -17.7 dBm (a more conservative value). In [19], a 100 Gbps PR-PAM-4 is tested using a 131-taps FFE, SOA+PIN and 25G-OE. A BtB sensitivity of -15 dBm is obtained at BER_T=10^{-2}. In contrast, we obtained a -19.3 dBm BtB sensitivity under similar conditions. A key difference between the referred work and our present manuscript, is the generation of the PR-PAM-4 signal. As explained before, we sent a pre-coded 4-level signal taking advantage of the intrinsic 25G-OE BW limitations to generate the 7-level signal at the RX side. Instead, in [19] the pre-coded 4-level signal is filtered by a 5th order Bessel filter with f_{3dB}=0.3R_S at the TX side, thus transmitting a 7-level signal that is filtered again by the O/E communication system. As shown in Fig. 4, over-filtering the PR-PAM-4 signal can result in considerable power penalties.

TABLE I. BtB achievable *OPL* in dB for different IM-DD scenarios, setting a transmitted power of P_{TX} = 11 dBm

		SOA+PIN		APD	
Format	RX Type	50G-OE	25G-OE	50G-OE	25G-OE
PAM-4	No EQ	32.5	N/A	29.9	N/A
	FFE	33.1	29.6	31.2	28.7
	DFE	33.1	30.1	31.2	29.4
PR-PAM-4	No EQ	26.6	29.8	25.1	28.7
	FFE	30.8	30.3	29.4	29.8
	DFE	31.1	30.3	29.6	29.7
PAM-8	No EQ	26.6	26.1	24.7	25.2
	FFE	28.8	28.5	27.9	28.0
	DFE	28.7	28.4	27.8	27.9

* N/A: Not Achievable.

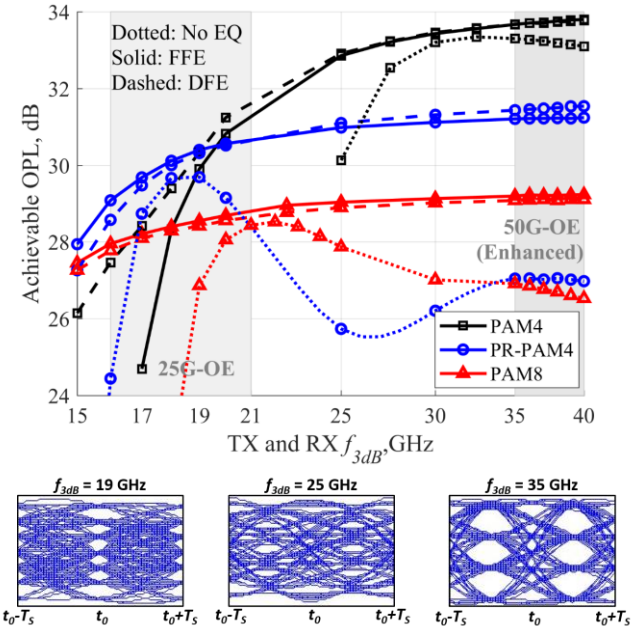

Fig. 4. Top: BtB achievable *OPL* (P_{TX}=11dBm) to get BER_T=10^{-2} versus TX and RX f_{3dB} (in log-scale) comparing different formats and digital receivers using SOA+PIN and setting in all cases the 25G-OE nominal parameters (thus, 50G-OE results are slightly enhanced). Bottom: received un-equalized PAM-4/PR-PAM-4 low-noise eye-diagrams showing two symbol periods (T_S) for three representative values of f_{3dB}, where t_0 is the initial sampling instant of one symbol (the PAM-4 and PR-PAM-4 eyes are identical at the equalizer input). Note: the optimum sampling instant (t_{OPT}) is around t_0 + 0.5·T_S for PAM-4, and always around t_0 for PR-PAM-4 (note that the un-equalized PAM-4 and PR-PAM-4 performance, in terms of achievable *OPL*, follows the eye-opening degree at t_{OPT} for the three f_{3dB} representative cases).

A summary of our reported IM-DD BtB results follows:

- Using 50G-OE, PAM-4 seems to be the best option (a gain of at least 2 dB with respect to PR-PAM-4 is obtained with AEQ), even without equalization (having only ~0.6 dB of penalty when avoiding it).

- Using 25G-OE, PR-PAM-4 outperforms the rest of the formats over a wide f_{3dB} range when using AEQ. If equalization is avoided, PR-PAM-4 still performs well but over a reduced f_{3dB} range (17-20 GHz).

4. TRANSMISSION OVER STANDARD SINGLE-MODE FIBER RESULTS

After having analyzed in BtB the impact of using O/E technology with different *BW* constraints in combination with digital solutions to counteract them, we now present our analysis including the effect of propagation through a conventional SMF. We start targeting O-band operation, thus preserving the IM-DD approach without dispersion pre-compensation. We then continue showing that this alternative reaches only around 5-km in C-band. Finally, we study two C-band alternatives that counteract dispersion from the TX side, keeping the RX with the same complexity as in the IM-DD architecture.

A. O-band operation (IM-DD without CD pre-compensation)

The dispersion values of the G.652 SMF O-band wavelength range currently considered for 50G-PON (1260 – 1344 nm) [4] span from D = -5 to 4 ps/nm·km (typical), resulting in an accumulated dispersion range of $D{\cdot}L$ = -100 to 80 ps/nm for a fiber length L=20 km. To evaluate the impact of CD in the performance of the IM-DD cases analyzed in previous Section 3, we computed the Required *ROP* to achieve the BER_T as a function of the accumulated dispersion. The obtained results are shown in Figures 5.a (50G-OE, SOA+PIN), 5.b (50G-OE, APD), 6.a (25G-OE, SOA+PIN) and 6.b (25G-OE, APD). Since the employed fiber model includes power-dependent Kerr non-linearities, we performed the simulations using as reference values a P_{TX}=11dBm [8] and a central λ=1342 nm (defined for the 50G-PON DS operation [4]). However, our reported results can be used to forecast the system performance when setting P_{TX} and λ values around the reference ones. Note that all the curves shown in Figures 5 and 6 are asymmetric with respect to the $D{\cdot}L$=0 value. The reason of this behavior is the well-known relation between Kerr nonlinear induced self-phase modulation (SPM) and dispersion [41]. SPM can partially compensate dispersion when D>0, whereas it worsen the CD impact when D<0. Therefore, for a same absolute value of D, a better performance is obtained if its sign is positive (i.e. the *RROP* curves are shifted towards positive $D{\cdot}L$ values).

A minimum *ROP* = -18 dBm is needed to achieve an *OPL* = 29 dB, setting a transmitted power of P_{TX}=11dBm. This *ROP* requirement can be met using different alternatives. One of them is 50G-OE operation with APD or SOA+PIN and using PAM-4 or PR-PAM4 with equalization (FFE is enough), showing feasibility over the -100 to 120 ps/nm range (see Fig. 5.b), covering the full λ = 1260 – 1344 nm range of operation from 0 to 20 km . Un-equalized PAM-4 with 50G-OE and SOA+PIN is also feasible over a reduced range of -60 to 90 ps/nm. Another interesting option is the re-use of 25G-OE with both SOA+PIN or APD in combination with PR-PAM-4 with equalization (FFE is enough), guaranteeing operation over $D{\cdot}L$ = -80 to 100 ps/nm. A fourth alternative is un-equalized PR-PAM-4 re-using 25G-OE with SOA+PIN receiver, achieving viability over $D{\cdot}L$ = -50 to 100 ps/nm.

Whereas the transmitted power is reduced to P_{TX}= 9 dBm [36] a *ROP* = -20 dBm is needed to guarantee an *OPL* = 29 dB. If small variations in the results presented in Figures 5 and 6 can be assumed when reducing the P_{TX} from 11 to 9 dBm, we can prognosticate that only by using the SOA+PIN 50G-OE option in combination with PAM-4 it is possible to achieve the *RROP*, over a $D{\cdot}L$=-70 to 100 ps/nm range (see Fig. 5.a). Un-equalized PAM-4 can also work in the same conditions, as long as $D{\cdot}L$ is within the -50 to 80 ps/nm range. Otherwise, the penalty starts increasing sharply. A summary of the feasible IM-DD options to achieve *OPL* = 29 dB over 20 km in the O-band is reported in Table II. Note that due to the aforementioned interaction between CD and Kerr-induced

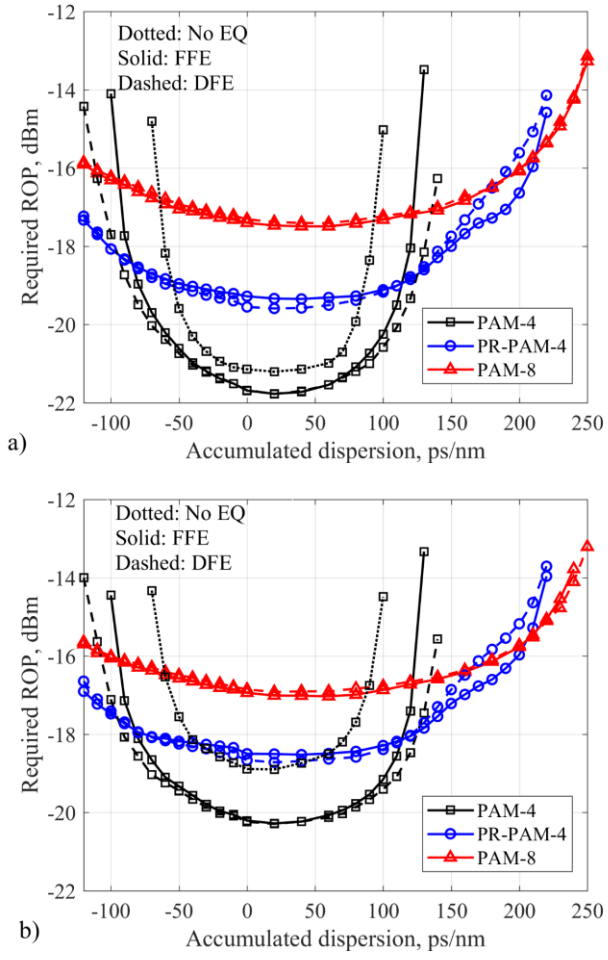

Fig. 5. *RROP* to get BER_T=10^{-2} as a function of accumulated dispersion (O-band, P_{TX}=11dBm) comparing different formats and digital RXs in combination with 50G-class O/E devices using a) a SOA+PIN and b) an APD. Note: among un-equalized cases, only PAM-4 is shown.

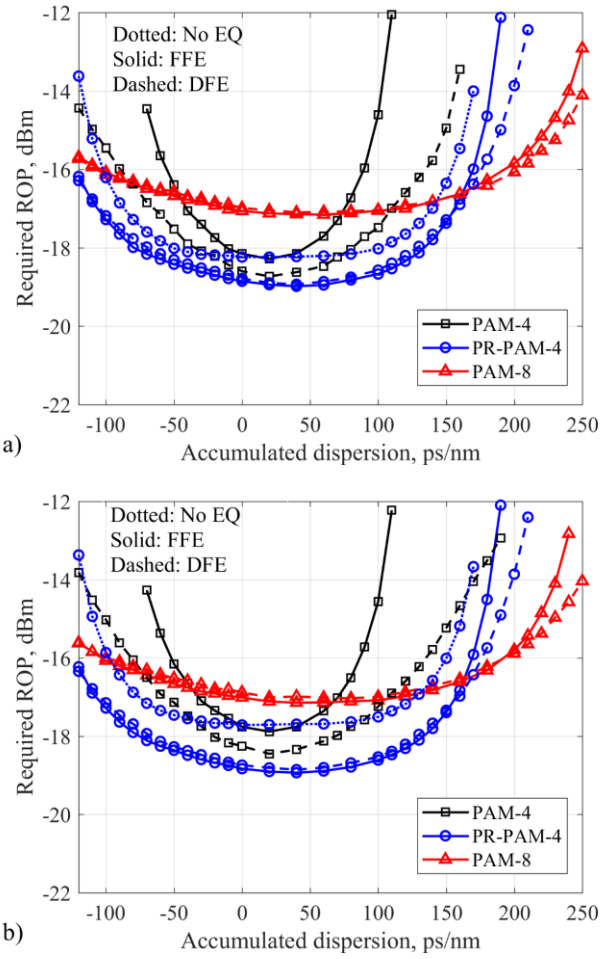

Fig. 6. *RROP* to get BER_T=10^{-2} as a function of accumulated dispersion (O-band, P_{TX}=11dBm) comparing different formats and digital RXs in combination with 25G-class O/E devices using a) a SOA+PIN and b) an APD. Note: among un-equalized cases, only PR-PAM-4 is shown.

SPM, the $D{\cdot}L$ feasible range is shifted towards positive values. Although not presented here for space limitations, it is well know that a given amount of chirp generated in the optical transmitter can move the *RROP* curves shown in Figures 5 and 6 towards the left or right in the $D{\cdot}L$ axis, as shown in [37] for 50G-PON. Therefore, it can be anticipated that a proper chirping management can help on slightly shifting the $D{\cdot}L$ range of operation from the values presented in Table II.

A 100G-PON system operating using PAM-4, APD and 25G-OE devices in O-band is reported in [8]. A sensitivity of -18.5 and -19.7 is achieved using 135-taps FFE and 135-taps FFE plus 30-taps DFE, respectively, obtaining a maximum *OPL* of 29.9 and 31.1 dB in each case, over 25-km and with a P_{TX}=11.4 dBm (the exact λ of operation is not reported). In this contribution we obtain -18 and -18.5 dBm under similar conditions (assuming λ ~ 1312 nm) using 20-taps FFE and 20-taps FFE plus 5-taps DFE, respectively. It is important to remark that tracking mode operation is considered here after training the equalizer with 10^4 symbols (the *BER* is evaluated excluding the part of the sequence used for training). Therefore, the DFE number of taps is kept reasonably low to avoid error propagation.

Among the analyzed formats, PAM-8 is the more resilient to dispersion, but also the one with the poorest sensitivity. Figures 5 and 6 anticipate that without CD pre-compensation, it is not possible to reach 20-km in C-band ($D{\cdot}L$ > 320 ps/nm) even if using PAM-8 plus DFE equalization. As mentioned in Section 1, other alternatives should then be used to extend the system operation to the C-band.

B. C-band operation (IM-DD versus CD-DPC-DD and IQ-DB-DD)

To take into account the λ-dependence of Kerr-nonlinearity, we replicate some of the IM-DD results presented in previous sub-section, but now in C-band with a reference λ = 1550 nm. They are shown in solid lines in Fig. 7.a, using SOA+PIN and 25G-OE. In this Figure, the achievable *OPL* as a function of the fiber length L is plotted for different IM-DD formats using DFE and setting P_{TX}=11 dBm. An *OPL* = 29 dB can be achieved only up to 5-km of fiber (using PR-PAM-4). A reduced *OPL* ~ 25 dB can be achieved using PAM-8 up to 11-km.

In order to extend the C-band reach, we use the CD-DPC-DD architecture described in sub-section 2.A.2 and detailed in [9, 29]. At the CD-DPC TX filter, the accumulated dispersion corresponding to L_C = 10 km was digitally pre-compensated (L_C stands for digitally pre-compensated fiber length). The driving signal amplitude was optimized for 10-km operation around the maximum *OPL*, and then set fixed for the rest of the *OPL*s and fiber lengths. The obtained results using CD-DPC-DD and PAM-4, PR-PAM-4 and PAM-8 plus DFE, considering SOA+PIN and 25G-OE, are shown in dashed-lines in Fig. 7.a. Due to the aforementioned SPM and CD interaction [41], the *OPL* versus L curves are slightly shifted in the L-axis with respect to L=10 km. One important difference between CD-DPC-DD with respect to the IM-DD operation, is the extra non-linearity introduced by the IQ-MZM, which has to be tolerated to obtain higher OMI values (for the IM-DD approach linear operation with a fixed ER is assumed). For PAM-4 and PR-PAM-4, the maximum achievable *OPL* using CD-DPC-DD (obtained around L=10-km) is similar to that obtained with IM-DD in BtB. In contrast, PAM-8 is more affected by IQ-MZM non-linear behavior, showing a ~1.5 dB penalty with respect to the BtB (and a shape asymmetry with respect to L=10 km, attributed to this phenomenon). At the TX side, both PAM-4 and PR-PAM-4 are 4-level signals, whereas PAM-8 has 8-levels, thus being more sensitive to non-linear distortions.

As mentioned in sub-section 2.D, the transmitted power at the IQ-MZM output depends on the driving signals amplitude, being around P_{TX}=11 dBm for the V_{pp} values analyzed here. Under this condition, an *OPL* of at least 29 dB can be achieved using PAM-4 in the 7-12 km range, or PR-PAM-4 in the 7-14 km range. Due to the strong constraints of single-λ PON transmission at 50 Gbps and beyond, the introduction of lower *OPL* requirements, such as 27 and 25 dB, has been discussed in the standardization groups for future PON upgrades. According to Fig. 7.a, a target *OPL* = 27 dB and 25 dB can be met using PR-PAM4 in the 3.5 – 15 km range and PAM-8 in the 3 – 19.5 km range, respectively.

TABLE II. O-band IM-DD options to get an *OPL* ≥ 29dB over 0-20-km

IM-DD option				P_{TX}, dBm	$D{\cdot}L$ range ps/nm
Format	O/E	Optical RX	RX Type		
PAM-4	50G	SOA+PIN	No EQ	11	-60 to 90
			FFE or DFE	11	-100 to 120
			No EQ	9*	-50 to 80
			FFE or DFE	9*	-70 to 100
		APD	No EQ	11	-40 to 60
			FFE or DFE	11	-90 to 110
	25G	SOA+PIN	DFE	11	-40 to 60
		APD	DFE	11	-30 to 60
PR-PAM-4	50G	SOA+PIN	FFE or DFE	11	-100 to 140
		APD	FFE or DFE	11	-80 to 120
	25G	SOA+PIN	No EQ	11	-50 to 100
			FFE or DFE	11	-80 to 130
		APD	FFE or DFE	11	-70 to 130

* Forecasted from the results obtained using P_{TX} = 11dBm.

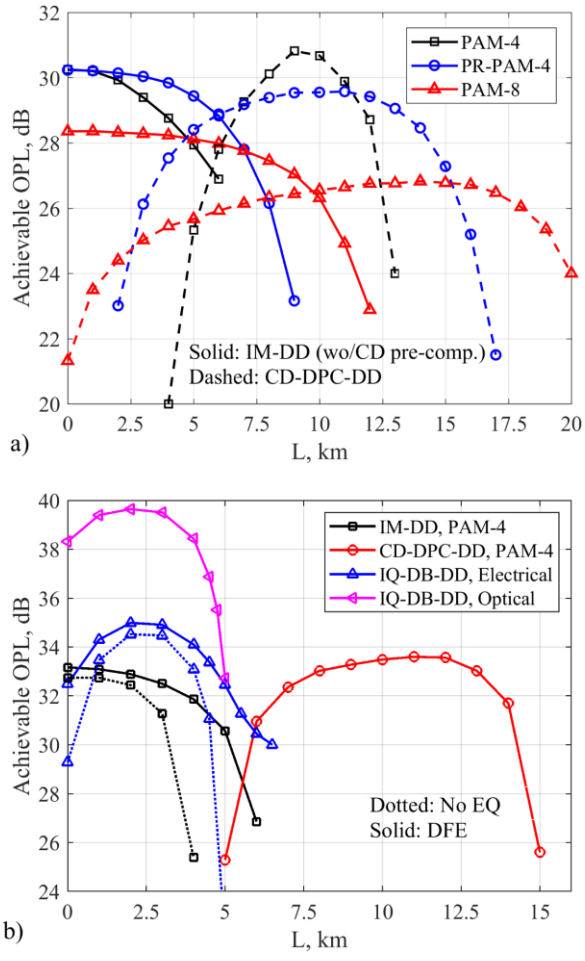

Fig. 7. Achievable *OPL* to get BER_T=10^{-2} as a function of fiber length (C-band at 1550 nm, P_{TX}~11dBm) using a SOA+PIN, comparing different formats and TX architectures in combination with a) 25G-class O/E devices + DFE, and b) 50G-class O/E devices and different digital RXs.

The CD-DPC-DD option is also tested using broadband 50G-OE technology, SOA+PIN receiver, in combination with PAM-4 plus DFE. The obtained *OPL* versus *L* curve is depicted in red with circles in Fig. 7.b. IM-DD PAM-4 results obtained under the same channel conditions are also shown for the sake of comparison (see squared black curves). Using CD-DPC-DD, an *OPL* of 29 and 25 dB can be achieved for distance ranges of 6-14 km and 5-15km, respectively.

From Fig. 7 we can observe that the maximum reach can be extended using the CD-DPC technique. However, the target *OPL* is not achieved in the full 0 to 20 km fiber range, thus not fulfilling a key requirement for Time Division Multiplexing (TDM)-PON operation: to serve several ONUs, each one located at a different arbitrary distance from the OLT. In contrast, the aforementioned issue is not a limitation to apply the CD-DPC-DD system on PtP- or WDM-PON C-band applications (such as future high-capacity fronthaul systems) where a dedicated lambda per ONU is used. In this case, TDM among different ONUs is not needed, so the CD pre-compensation can be set on an ONU by ONU base. Moreover, the CD-DPC-DD curves shown in Fig. 7 can be "shifted" to longer fiber length targets, with a marginal maximum *OPL* penalty, by just changing the pre-compensated fiber length L_C [29], enabling long-reach systems supporting high *OPL* at a given target distance. To enable TDM-PON DS operation, the CD pre-compensation should be specific for the data sent to a given ONU (thus reaching many ONUs by using the proper pre-compensation value $D{\cdot}L_i$, where L_i is the estimated fiber distance to ONU$_i$). One alternative discussed in [9] is based on FIR filters able to adapt dynamically by changing its taps (from a pre-computed set) depending on the target ONU$_i$-to-OLT distance L_i. This solution requires an estimation of each L_i, which can be obtained with enough accuracy by using similar PON ranging algorithms as those used in XGS-PON [29]. However, in order to perform L_i estimation, initial communication between the ONU and the OLT should be guaranteed in the discovery stage. Since at the beginning L_i is unknown, the CD-DPC technique should be turned-off performing the discovery algorithm at a lower bit rate (for instance, 10 Gbps as in XGS-PON) to guarantee C-band uncompensated correct operation [29]. We are currently further studying all these details needed for TDM-PON 100G-PON DS based-on a CD-DPC-DD system.

Finally, the IQ-DB-DD solution is tested in C-band, using 50G-OE and SOA+PIN. IQ-DB modulation (in both electrical and optical versions), is performed by encoding a bit sequence to produce a duobinary complex one with $R_S = R_b$, i.e. 100 GBd. A poor sensitivity is then anticipated using 25G-OE, so that we did not analyze this option. At the TX side, IQ-DB-DD requires the same DSP sampling rate as CD-DPC-DD with PAM-4 (or PR-PAM-4), since the signal processing is performed at just 1 SpS (see Fig. 1). However, the IQ-DB-DD RX DSP is performed at 2 SpS if AEQ is included, thus requiring twice the RX DSP speed of CD-DPC-DD using PAM-4 (i.e. 200 GS/s). One alternative to avoid this high DSP rate, is not performing RX equalization. In the IQ-DB-DD electrical version, the RX signal is a 3-level DB one, therefore is expected to work without AEQ and 50G-OE. In contrast, in the IQ-DB-DD optical version a binary 100 Gbps signal is received directly after photo-detection, thus anticipating a bad performance without AEQ if using 50G-OE.

Following the previous discussion, three IQ-DB-DD cases are analyzed and plotted in Fig. 7.b: optical version with DFE, electrical version with DFE and electrical version without AEQ (this last option requires the simplest ONU RX among all the analyzed solutions of this contribution). The IQ-DB-DD design parameters β and ρ (see sub-section 2.A.3) are set equal to 1/3 and 0.275, respectively [24, 25]. The V_{pp} is optimized to achieve the maximum reach at *OPL* = 29 dB, and then keep fixed for the rest of the fiber lengths. Fig. 7.b shows that the three IQ-DB-DD cases outperforms the corresponding PAM-4 IM-DD options, increasing both the fiber reach and the maximum achievable *OPL* (at the expense of requiring twice the DSP RX speed when using AEQ). However, the C-band reach obtained with IQ-DB-DD alternatives is at most 7-km (~120 ps/nm), thus being a more suitable solution for other high-speed short-reach solutions or for 100G-PON O-band applications with a high *OPL* and accumulated dispersion requirements. For the sake of comparison, an un-equalized IQ-DB-DD solution was shown able to reach 17-km in an experimental 50 Gbps C-band transmission [25]. Since the CD tolerance is reduced four times when doubling the bit rate, a 4.25-km reach at 100 Gbps can be forecasted from the aforementioned results, very close to the simulation results presented here (4.7-km reach without penalty with respect to the BtB) under similar conditions.

5. CONCLUSIONS AND DISCUSSION

Different 100G-PON downstream solutions were analyzed using 25G- and 50G-class optoelectronics technology, targeting to preserve direct-detection scheme and simple digital receivers. A comparison among the studied alternatives is summarized in Table III, in terms of performance, cost and complexity (these last two in a qualitative way). It is evident that to extend the 100G-PON operation to the C-band, the cost and complexity of the RX ONU can remain similar only at the price of significantly increasing the TX OLT ones (specially for the extra cost of including an IQ-MZM).

TABLE III. Comparison of the analyzed single-λ 100G-PON downstream solutions

Scheme	RX	O/E class	RX DSP	Operational range (Δ) to admit an *OPL*≥29dB:		O/E Devices Cost [5, 6, 15, 39, 40]		DSP Complexity [6, 15]	
				ΔL	$\Delta D{\cdot}L$ (see Table II)	ONU	OLT	ONU	OLT
IM-DD (O-band)	APD	25G	wo/EQ	N/A	N/A	★	★	★	★
			w/EQ	0–20 km [b]	-70–130 ps/nm [b]	★	★	★★	★
		50G	wo/EQ	0–20 km [a]	-40–60 ps/nm [a]	★★★	★★★	★	★
			w/EQ	0–20 km [a]	-90–110 ps/nm [a]	★★★	★★★	★★	★
	SOA +PIN	25G	wo/EQ	0–20 km [b]	-50–100 ps/nm [b]	★★	★	★	★
			w/EQ	0–20 km [b]	-80–130 ps/nm [b]	★★	★	★★	★
		50G	wo/EQ	0–20 km [a]	-60–90 ps/nm [a]	★★★★	★★★	★	★
			w/EQ	0–20 km [a]	-100–120 ps/nm [a]	★★★★	★★★	★★	★
CD-DPC-DD (C-band)	SOA +PIN	25G	w/EQ	7–14 km [b]	120–240 ps/nm [b]	★★	★★★★★	★★	★★★
		50G	w/EQ	6–14 km [a]	100–240 ps/nm [a]	★★★★	★★★★★★	★★	★★★
IQ-DB-DD (C-band)	SOA +PIN	50G	w/EQ	0–7.5 km [c]	0–130 ps/nm [c]	★★★★	★★★★★★	★★	★★
		50G	w/EQ	0–5 km [d]	0–85 ps/nm [d]	★★★★	★★★★★★	★★	★★

Modulation format: [a] PAM-4, [b] PR-PAM-4, [c] IQ-DB, Electrical, [d] IQ-DB, Optical; N/A: *OPL*=29dB not achievable even in BtB

In O-band, PAM-4 IM-DD solutions using 50G-class devices as well as PR-PAM-4 IM-DD alternatives using 25G-class devices, were shown to be feasible (*OPL* ≥ 29 dB) over 0 to 20 km of SMF and a wide range of operational wavelengths (even avoiding equalization under proper conditions).

In C-band, we showed that 100G-PON achieving *OPL* ≥ 29 dB over the full 0 to 20 km length range is very challenging if wanting to keep the RX complexity low. 100G-PON applications with relaxed *OPL* requirements, and/or reduced differential fiber length, can be feasible in C-band using the proposed CD-DPC-DD architecture, adding some complexity to the OLT TX but still keeping the same ONU RX complexity as the IM-DD approaches.

Finally, using the downstream results presented here as a baseline, preliminary considerations about the 100G-PON US direction can be discussed. First, the "complexity path" should be reversed, in the sense that extra complexity can be placed at the RX side (i.e. at the OLT) maintaining as simple as possible the ONU TX. From the results presented in this contribution, an IM-DD architecture, including equalization at RX, can be forecasted to work in the O-band for the US direction, under a reduced range of operational wavelengths accounting for an extra power penalty due to burst-mode operation. In C-band, CD compensation was shown to be a must to achieve the 0 – 20 km reach. One C-band US alternative able to perform this compensation at the RX is to use burst-mode coherent detection at the OLT [10, 12, 13], in combination with a conventional IM transmitter [11] to keep simple the ONU.

Acknowledgment. This work was carried out under the PhotoNext initiative at Politecnico di Torino (http://www.photonext.polito.it/) and inside a research contract with Telecom Italia (TIM).

References

1. *IEEE Standard for Ethernet Amendment 9: Physical Layer Specifications and Management Parameters for 25 Gb/s and 50 Gb/s Passive Optical Networks*, in IEEE Std 802.3ca-2020, pp. 1-267, 2020.
2. ITU-T, "G.Sup64 PON transmission technologies above 10 Gbit/s per wavelength", 2018.
3. E. Harstead, D. van Veen, V. Houtsma, P. Dom, "Technology Roadmap for Time-Division Multiplexed Passive Optical Networks (TDM PONs)," Journal of Lightwave Technology, vol. 37, no. 2, pp. 657-664, 2019.
4. D. Zhang, D. Liu, X. Wu, D. Nesset, "Progress of ITU-T higher speed passive optical network (50G-PON) standardization," J. Opt. Commun. Netw. 12, D99-D108, 2020
5. E. Harstead, R. Bonk, S. Walklin, D. van Veen, V. Houtsma, N. Kaneda, A. Mahadevan, R. Borkowski, "From 25 Gb/s to 50 Gb/s TDM PON: transceiver architectures, their performance, standardization aspects, and cost modeling," J. Opt. Commun. Netw. 12, D17-D26, 2020.
6. D. van Veen, V. Houtsma, "Strategies for economical next-generation 50G and 100G passive optical networks [Invited]," J. Opt. Commun. Netw. 12, A95-A103, 2020.
7. J. Zhang, J. Yu, J. Shan Wey, X. Li , Li Zhao, K. Wang, M. Kong, W. Zhou, J. Xiao, X. Xin, F. Zhao, "SOA Pre-Amplified 100 Gb/s/λ PAM-4 TDM-PON Downstream Transmission Using 10 Gbps O-Band Transmitters," J. Lightwave Technol., vol.38, pp. 185-193, 2020.
8. S. Luo, Z. Li, Y. Qu, Y. Song, J. Chen, Y. Li, M. Wang, "112-Gb/s/l Downstream Transmission for TDM-PON with 31-dB Power Budget using 25-Gb/s Optics and Simple DSP in ONU," in Proc. Optical Fiber Communication Conference (OFC), 2020, paper Th3K.4
9. P. Torres-Ferrera, V. Ferrero, R. Gaudino, "100 Gbps PON L-band Downstream Transmission using IQ-MZM CD Digital Pre-Compensation and DD ONU receiver," in Proc. Optical Fiber Communication Conference (OFC), 2020, paper Th1B.1.
10. R. Matsumoto, K. Matsuda, N. Suzuki, "Burst-Mode coherent detection using fast-fitting pi lot sequence for 100-Gb/s/λ coherent TDM-PON systems," in Proc. Eur. Conf. Opt. Commun. (ECOC), 2017, Paper W.3.D.5
11. J. Zhang, J. Shan Wey, J. Shi, J. Yu, "Single-wavelength 100-Gb/s PAM-4 TDM-PON achieving over 32-dB power budget using simplified and phase insensitive coherent detection," in Proc. Eur. Conf. Opt. Commun. (ECOC), 2018, Paper Tu1B.1
12. N. Suzuki, H. Miura, K. Matsuda, R. Matsumoto, K. Motoshima, "100 Gb/s to 1 Tb/s based coherent passive optical network technology," J. Lightw. Technol., vol. 36, no. 8, pp. 1485–1491, 2018.
13. J. Zhang, Z. Jia, M. Xu, H. Zhang, L. A. Campos, C. Knittle, "High-Performance Preamble Design and Upstream Burst Mode Detection in 100 -Gb/s/λ TDM Coherent-PON," in Proc. Optical Fiber Communication Conference (OFC), 2020, paper W1E.1.
14. J. Zhang, Z. Jia, H. Zhang, M. Xu, J. Zhu, L. A. Campos, "Rate-Flexible Single-Wavelength TFDM 100G Coherent PON based on Digital Subcarrier Multiplexing Technology," in Proc. Optical Fiber Communication Conference (OFC), 2020, paper W1E.5
15. Y. Zhu, L. Yi, B. Yang, X. Huang, J. Shan Wey, Z. Ma, W. Hu, "Comparative study of cost-effective coherent and direct detection schemes for 100 Gb/s/λ PON," J. Opt. Commun. Netw. 12, D36-D47, 2020.
16. L. Yi, P. Li, T. Liao, W. Hu, "100 Gb/s/λ IM-DD PON using 20G class optical devices by machine learning based equalization," in Proc. Eur. Conf. Opt. Commun. (ECOC), 2018, Paper Mo4B.5
17. L. Yi, T. Liao, L. Huang, L. Xue, P. Li, W. Hu, "Machine Learning for 100 Gb/s/λ Passive Optical Network," J. Lightwave Technol. vol. 37, pp. 1621-1630, 2019.
18. V. Houtsma, E. Chou, D. van Veen, "92 and 50 Gbps TDM-PON using Neural Network Enabled Receiver Equalization Specialized for PON," Proc. Optical Fiber Communication Conference (OFC), 2019, paper M2B.6.
19. M. G. Saber, D. V. Plant, R. Gutiérrez-Castrejón,M. S. Alam, Z. Xing, E. El-Fiky, L. Xu, F. Cavaliere, G. Vall-Llosera, S. Lessard, "100 Gb/s/ λ Duo-Binary PAM-4 Transmission Using 25G Components Achieving 50 km Reach," IEEE Photonics Technology Letters, vol. 32, no. 3, pp. 138-141, 2020.
20. R. Gaudino, P. Torres-Ferrera, H. Wang, M. Valvo, A. Pagano, R. Mercinelli, V. Ferrero, "Opportunities and Challenges When Using Low Bandwidth Optics for Higher Capacity PON Systems (Invited paper)," in Proc. Optical Fiber Communication Conference (OFC), 2020, paper Th3K.5.
21. P. Torres-Ferrera, V. Ferrero, M. Valvo, R. Gaudino, "Impact of the Overall Electrical Filter Shaping in Next-Generation 25 and 50 Gb/s PONs", Journal of Optical Communications and Networking, vol. 10, no. 5, pp. 493-505, 2018.
22. P. Torres-Ferrera, H. Wang, V. Ferrero, M. Valvo, R. Gaudino, "Optimization of Band-Limited DSP-Aided 25 and 50 Gb/s PON Using 10G-Class DML and APD," J. Lightwave Technol., vol. 38, pp. 608-618, 2020.
23. E. Forestieri, G. Prati, "Novel Optical Line Codes Tolerant to Fiber Chromatic Dispersion," J. Lightwave Technol. 19, 1675, 2001.
24. E. Forestieri, M. Secondini, F. Fresi, G. Meloni, L. Potí, F. Cavaliere, "Extending the Reach of Short-Reach Optical Interconnects With DSP-Free Direct Detection," J. Lightwave Technol. 35, 3174-3181, 2017.
25. M. Morsy-Osman, F. Fresi, E. Forestieri, M. Secondini, L. Potì, F. Cavaliere, S. Lessard, D. V. Plant, "50 Gb/s short-reach interconnects with DSP-free direct-detection enabled by CAPS codes," Opt. Express 26, 17916-17926, 2018.
26. R. I. Killey, P. M. Watts, V. Mikhailov, M. Glick, P. Bayvel, "Electronic dispersion compensation by signal predistortion using digital processing and a dual-drive Mach–Zehnder modulator," IEEE Photonics Technol. Lett. 17(3), 714–716, 2005.
27. Q. Zhang, N. Stojanovic, C. Xie, C. Prodaniuc, P. Laskowski, "Transmission of single lane 128 Gbit/s PAM-4 signals over an 80 km SSMF link, enabled

by DDMZM aided dispersion pre-compensation," Opt. Express 24, 24580-24591, 2016.
28. J. Zhang, J. Yu, J. Shi, J. S. Wey, X. Huang, Y. Guo, Z. Ma, M. Li, "64-Gb/s/A Downstream Transmission for PAM-4 TDM-PON with Centralized DSP and 10G Low-Complexity Receiver in C-Band," in Proc. Eur. Conf. Opt. Commun. (ECOC), pp. 1-3, Gothenburg, 2017.
29. P. Torres-Ferrera, G. Rizzelli, V. Ferrero, R. Gaudino, "100+ Gbps/λ 50km C-band Downstream PON using CD Digital Pre-Compensation and Direct-Detection ONU Receiver," J. Lightwave Technology, doi: 10.1109/JLT.2020.3021897, 2020.
30. X. Chen, C. Antonelli, S. Chandrasekhar, G. Raybon, A. Mecozzi, M. Shtaif, P. Winzer, "Kramers–Kronig Receivers for 100-km Datacenter Interconnects," J. Lightwave Technology, 36, pp. 79-89, 2018.
31. H. Faig, B. V. Pedersen, S. Cohen, L. Gantz, D. Sadot, "Nonlinear System Identification Scheme for Efficient Compensators Design," J. Lightwave Technology, vol. 38, no. 13, pp. 3519-3525, 2020.
32. A. Lender, "Correlative digital communication techniques," IEEE Transactions on Communication Technology, vol. 12, no. 4, pp. 128–135, 1964.
33. N. Stojanovic, Z. Qiang, C. Prodaniuc and F. Karinou, "Performance and DSP complexity evaluation of a 112-Gbit/s PAM-4 transceiver employing a 25-GHz TOSA and ROSA," in Proc. Eur. Conf. Opt. Commun. (ECOC), pp. 1-3, Valencia, 2015.
34. J. Goergen, "The Reality of Channels Operating at 100Gbps," IEEE802.3 Meeting, 24 May 2017, New Orleans, 2017. [Online] Available: https://www.ieee802.org/3/ad_hoc/ngrates/public/17_05/goergen_nea_01_0517.pdf
35. M. Chagnon, "Optical Communications for Short Reach," J. Lightw. Technol, 37 (8), pp. 1779-1797, 2019.
36. T. Shindo, N. Fujiwara, S. Kanazawa, M. Nada, Y. Nakanishi, T. Yoshimatsu, A. Kanda, M. Chen, Y. Ohiso, K. Sano, H. Matsuzaki, "High Power and High Speed SOA Assisted Extended Reach EADFB Laser (AXEL) for 53-Gbaud PAM4 Fiber-Amplifier-Less 60-km Optical Link," J. Lightwave Technol. 38, 2984-2991, 2020.
37. R. Borkowski, H. Schmuck, G. Cerulo, J. Provost, V. Houtsma, D. van Veen, E. Harstead, F. Mallecot, and R. Bonk, "The Impact of Transmitter Chirp Parameter on the Power Penalty and Design of 50 Gbit/s TDM-PON," in Proc. Optical Fiber Communication Conference (OFC), 2020, paper Th1B.5.
38. K. Zhang, Q. Zhuge, H. Xin, W. Hu, D. V. Plant, "Performance comparison of DML, EML and MZM in dispersion-unmanaged short reach transmissions with digital signal processing," Opt. Express 26, 34288-34304, 2018.
39. J. Turkiewicz, "Cost-effective n × 25 Gbit/s DWDM transmission in the 1310 nm wavelength domain," Optical Fiber Technology 17(3), pp. 179-184, 2011.
40. D. Lee, B. Y. Yoon, "Optic Cost Estimation for 10G EPON Downstream," IEEE 802.3av 10Gb/s EPON TF, San Francisco, CA, July 2007. [Online] Available: https://www.ieee802.org/3/av/public/2007_07/3av_0707_lee_1.pdf
41. Z. Chen, L. Yan, W. Pan, B. Luo, X. Zou, H. Jiang, "A Transmission Model of Analog Signals in Photonic Links," IEEE Photonics Journal, vol. 6, no. 6, pp. 1-13, 2014.

Pablo Torres-Ferrera received the B.Eng., M.E.E. and Ph.D. degrees (with honors) in telecommunications in 2010, 2012 and 20 17, respectively, from the National Autonomous University of Mexico (UNAM), Mexico City. He worked from 2012 to 2013 at Huawei Technologies Mexico in the implementation of OTN rings. As part of his PhD investigation work, he carried out research internships at Athens Information Technology (AIT), Greece, in 2014 and at Politecnico di Torino, Italy, in 2016. Since 2017, he is a Post-Doctoral Researcher at Politecnico di Torino, working in the field of high-speed optical access networks and data-center interconnects.

Haoyi Wang received the bachelor degree in Telecommunication Engineering in 2015, and the master degree in Communication and Computer Networks Engineering in 2018, both from Politecnico di Torino, Italy. Now, she is a Ph.D. candidate in Electrical, Electronics and Communication Engineering at Politecnico di Torino. Her current research interest includes the area of high-speed optical access networks.

Valter Ferrero received the Laurea degree (summa cum laude) in Electronics Engineering in 1994 from Politecnico di Torino, Italy. In 1994, he collaborated with Politecnico di Torino, working on coherent optical systems. From 1995 to 1996, he was with GEC Marconi (now Ericson), Genova, Italy. In 1997, he was in charge of the Optical Laboratory, Department of Electrical Engineering, Politecnico di Torino. He is Associate Professor, author or co-author of more than 80 papers in the field of Optical Communications. He is currently with the Optical Communications Group, Politecnico di Torino. His current research interests include optical coherent communications, free-space optical communications, and next-generation passive optical networks.

Roberto Gaudino Ph.D., is Full Professor at Politecnico di Torino, Italy. His main research interests are in the long haul DWDM systems, fiber non-linearity, modelling of optical communication systems and in the experimental implementation of optical networks, with specific focus on access networks. In particular, in the last five years, he focused his activity on short-reach optical links using plastic optical fibers (POF) and on next-generation passive optical access networks (NG-PON2). Currently, he is working on ultra-high capacity systems for medium reach links. Previously, he worked extensively on fiber modelling, optical modulation formats, coherent optical detection, and on the experimental demonstration of packet switched optical networks. He is author or co-author of more than 200 papers in the field of Optical Communications. From 2009 to 2016 he was the coordinator of three projects in the area of optical access (EU FP6-IST STREP "POF-ALL" and "POF-PLUS" and EU FP7-ICT STREP project "FABULOUS"). He is now the coordinator of the PhotoNext center at POLITO.